Extraction of Pyrocatechol from pharmaceutical wastewater through Adsorption Using Molecularly Imprinted Polymer prepared from Methacrylic Acid Monomer

K. N. Awokoya[1]*, V. O. Oninla[1] and M. A. Bakare[1]

[1]Department of Chemistry, Obafemi Awolowo University, Ile-Ife, Osun State, Nigeria

*Corresponding author: knawokoya@gmail.com Tel**:** +234 803 419 9393

Abstract

Development of inexpensive adsorbents from polymer materials for the extraction of pyrocatechol (PC) from wastewaters is an important area in environmental sciences. The study involves the development of molecularly imprinted polymer (MIP) as sorbent material for the extraction of PC from wastewater. To realize this objective, the non-covalent approach has been applied for the preparation of MIP using methacrylic acid (MAA) as a functional monomer and ethylene glycol dimethacrylate (EGDMA) as crosslinker. Furthermore, the synthesized polymers were characterized by Fourier-transform infrared spectroscopy (FTIR), scanning electron microscopy (SEM) and X-ray diffraction (XRD) analysis techniques. Adsorption equilibrium data were determined for the uptake of PC from synthetically prepared aqueous PC solution. The designed MIP demonstrated outstanding affinity towards PC. The adsorption capacity of the MIP increases from 1.91 to 27.60 mg/g by increasing the initial concentration of PC from 10 to 500 mg/L, yielding a hyperbolic curve. The equilibrium data were evaluated using two isotherm models namely, Langmuir and Freundlich isotherms. The MIP material was used for extraction of PC from real sample of pharmaceutical effluent and its efficiency was studied.

Keywords: Molecular imprinting, adsorption, pyrocatechol, wastewater, characterization

1. Introduction

Pyrocatechol is a phenolic compound, and generally considered as one of the most hazardous industrial pollutant in pesticides and pharmaceutical wastewater. Phenolic compounds are common industrial pollutants and they are highly toxic even at low concentrations [1]. They are discharged as industrial effluents from rubber, pesticide-making, textiles, paper, dye, petrochemical, plastic, petroleum refinery, pharmaceutical and fragrance industries [2-6]. Due to their perceivable toxicity and actions upon aquatic organisms including bioaccumulation in fish, the Environmental Protection Agency (EPA) has identified more than one hundred compounds as organic pollutants [7]. For example, phenol and its derivatives such as hydroquinone, chlorophenols, nitrophenols and pyrocatechol etc have been registered as priority pollutants by US Environmental Protection Agency [8]. Hence, removal of phenolic compounds such as pyrocatechol from aqueous media is of great importance.

There are various methods based on chemical and physical processes that have recently been applied for phenolic compounds removal like membrane extraction, distillation, adsorption, ozonation and electrochemical methods [9]. Among them, adsorption technology has been the most frequently applied method, and still is the most economic nondestructive process. Many attempts have been made by researchers to develop adsorbents for removal of organic pollutants. The reported adsorbents include zeolite-based materials, activated carbons, metal oxides, metal sulfide, and so on [10-11]. However, most of these adsorbents are not quite

efficient in terms of selectivity. To selectively remove pyrocatechol from aqueous media, molecular imprinting technology is considered to be an efficient and economic method.

Molecular imprinting is an efficient technique for the preparation of molecularly imprinted polymers (MIPs) with specific recognition cavities complementary to the template molecules in shape, size and functional groups [12]. Principal materials that have to be well chosen in preparation of MIP are crosslinking agents, template molecules, porogenic solvents, initiators and functional monomers. Functional monomer selection and template design are two of the most critical features of the molecular imprinting process [13-14]. In addition, the careful choice of functional monomer is one of the utmost importance to provide integrative interactions with the template. From the usual mechanism pattern of formation of MIP recognition properties, functional monomers are responsible for the recognition interactions in the imprinted recognition sites. It is very crucial to match the functionality of the functional monomer with the functionality of the template in an integrative fashion in order to achieve a very good imprint [15]. Also, it has been established that number and quality of molecularly imprinted polymer recognition sites is a direct function of the mechanisms and extent the monomer-template interactions present in the prepolymerisation mixture [16]. In view of this, in the last four decades, the use of many functional monomers has been studied in non-covalent imprinting [17-19]. There are categories of functional monomers, namely, acidic, basic and neutral monomers. In this present work, a new pyrocatechol imprinted polymer has been synthesized using acidic functional monomer.

The main purpose of this study was to prepare methacrylic acid based imprinted polymer crosslinked with ethyleneglycol dimethacrylate with pyrocatechol as template to improve stability, the adsorption ability and selectivity of the imprinted sorbent toward pyrocatechol. Moreover, the characteristic properties of the methacrylic acid based imprinted polymer with pyrocatechol in aqueous solution was investigated via

characterization of Fourier transform infrared (FTIR) spectroscopy, Scanning electron microscopy (SEM) and Powder X-ray diffraction (XRD). To the best of the authors' knowledge, there are no reports in the open literature on the effectiveness of methacrylic acid based imprinted polymer for removal of pyrocatechol from aqueous media.

2. Experimental

2.1 Materials and reagents

Methacrylic acid (MAA), ethylene glycol dimethacrylate (EGDMA), pyrocatechol (PC), azobisisobutyronitrile (AIBN), were supplied by Sigma-Aldrich, Germany and used as obtained. Methanol (MeOH), chloroform and acetic acid were supplied by Majog chemicals (Nigeria). Distilled water was supplied by Department of Chemistry, Obafemi Awolowo University, Nigeria. All chemicals used were of analytical grade. All the adsorption measurements were carried out using a UV-vis spectrophotometer (Schimadzu, UV-1800, USA).

2.2 Preparation of Molecularly Imprinted Polymer

The method of Awokoya *et al* (2013) was used with a slight medication [20]. The pyrocatechol MIPs were prepared by bulk polymerization using PC, MAA, EGDMA and AIBN as template molecule, functional monomer, crosslinker and initiator, respectively. PC (400 mg, 3.63 mmol), MAA (1.6 mL, 18.96 mmol), EGDMA (17.5 ml, 92.79 mmol), and AIBN (5 mg, 0.02 mmol) were placed in chloroform (1.2 mL, 14.9 mmol) in a standard flask (scheme 1). The mixture was stirred, and transferred into a heating module. The temperature was increased from room temperature to 70 ^{O}C within 30 min, and then kept at 70 ^{O}C for 72 h. After polymerization process, the glass tube was broken and the resulting MIPs (brown solid polymers) was wiped free of the broken glass and the monolith was ground with a mortar and pestle. As control, a non imprinted polymer (NIP) was also prepared following the same procedure, except that the template molecule was omitted from the polymerization process. Schematic of preparing MIP, with PC as template in chloroform, MAA as

functional monomer, EDGMA as crosslinker and AIBN as initiator is shown in Scheme 1.

2.3 Template Removal

The method of Awokoya *et al* (2013) was used with a slight medication [20]. To remove the template molecule, the polymer was exhaustively washed and stirred magnetically for 2.5 h with a mixture of MeOH and acetic acid (90:10, v/v). The cooled reaction mixture was centrifuged and the supernatant liquids were tested until no pyrocatechol was observed to leach from the polymer using a UV-vis spectrophotometer. Then, the polymer was washed several times with pure MeOH to remove the acetic acid and facilitate drying.
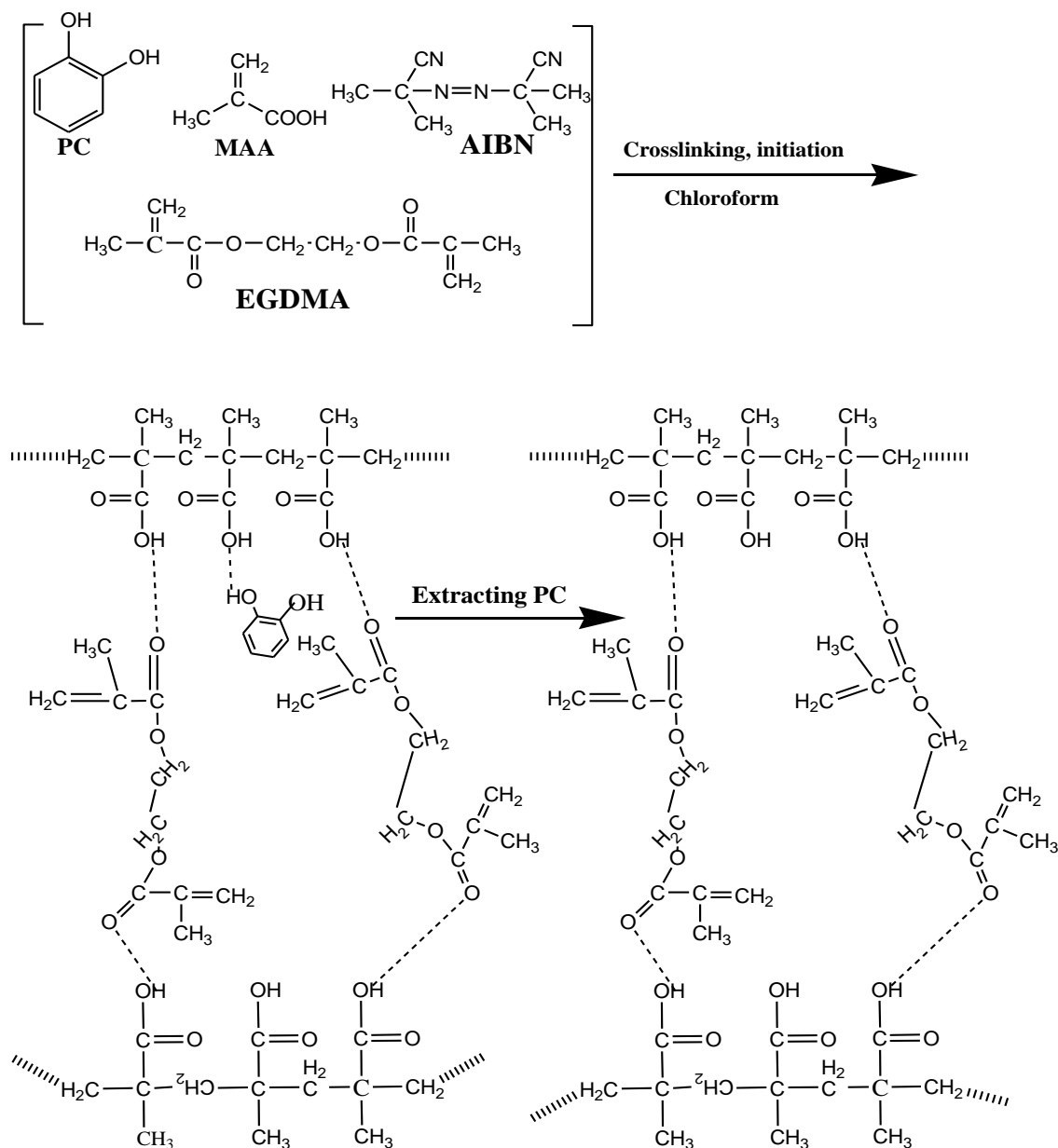
Scheme 1. Synthesis of MIP with PC as template, MAA as functional monomer, EDGMA as crosslinker and AIBN as initiator.

2.4 Scanning Electron Microscopy (SEM)

3

Morphologies of the MIP and NIP particles were studied using a concise FEGSEM 6100 Zeiss ultra Plus Germany at an accelerated voltage of 20.0 kV with secondary electrons in low vacuum mode (LV). Prior to the SEM analysis, the samples were taken and dusted onto a carbon sticker, then coated with gold using a sputter coater for 30 min and then the images were recorded.

2.5 Fourier Transform Infrared (FT-IR) Spectroscopy

The Fourier transform infrared (FT-IR) spectra of the MIP and NIP particles were obtained using impact 330 series Nicolet Avatar FT-IR spectrometer model in the frequency range $4000 - 650$ cm^{-1} using potassium bromide disks.

2.6 X-ray Powder Diffraction (XRD)

To get an insight into the structure of imprinted and non-imprinted polymers formed by using methacrylic acid functional monomer, powder XRD patterns were recorded using an X-ray diffractometer BRUKER D2 PHASER DOC-M88-EXX155 V4-07, 2010 Germany, using the Cu tube with 1.5418 (Å) radiation. Data were recorded during 2Θ range of 10°-90° under continuous scan mode using the scan rate of 4°/min.

2.7 Adsorption Studies

The adsorption experiment of pyrocatechol unto MIP was performed at room temperature by adding an optimal quantity of the washed MIP (100 mg) into 20 mL of chloroform with initial concentrations of chloroform ranging from 10 to 500 mg/L. After shaking for 6 h, MIPs were separated by centrifugation at 6000 rpm for 10 min, and the concentration of PC in the mixed solution was determined by UV-vis spectrophotometer. The adsorption capacity (Q$_e$ mg/g) was calculated before and after the adsorption according to Eq. 1:

$$Q_e = \frac{(C_o - C_e)V}{W} \qquad 1$$

Adsorption studies were carried out on both samples using 100 mg of MIP/NIP as previously described in the adsorption protocol. The concentrations of the PC

Where C$_o$ is the initial PC concentration (mg/L) and C$_e$ is the PC concentration at adsorption equilibrium (mg/L), V is the volume of PC solution, and W is the weight of the MIP or NIP (g).

Many theoretical and empirical models have been developed over the years to represent the various types of adsorption isotherms. As of now, there is no single model that suitably describes all mechanisms and shapes. Among the isotherms, Langmuir and Freundlich models have been broadly used. The adsorption capacity values were evaluated using Langmuir equation (Eq. 2) and Freundlich equation (Eq. 3) [21-22].

$$\frac{C_e}{Q_e} = \frac{C_e}{Q_m} + \frac{1}{(K_a \, Q_m)} \qquad 2$$

$$\log Q_e = \log K_f + \frac{1}{n} \, log C_e \qquad 3$$

where C_e (mg/L) and Q_e (mg/g) are PC concentration and adsorption capacity at adsorption equilibrium, respectively, and Q_m (mg/g) and K_a (L/mg) are the theoretical maximum adsorption capacity and Langmuir equilibrium constant related to the theoretical maximum adsorption capacity and energy of adsorption, respectively. K_f and n are the Freundlich constants that are indicators of adsorption capacity and adsorption intensity, respectively. K_f and n can be determined from a linear plot of $log Q_e$ against $log C_e$.

2.8 Method validation using real effluent

Batch extractions were performed using n-butanol as solvent in the extraction of PC. Real effluent (30 mL) from pharmaceutical industry and n-butanol (30 mL) were taken in a beaker and was agitated for 30 min. After agitation, the mixture was transferred to a separating funnel for settling. The extract was then decanted from the separating funnel into a 50 mL beaker. Two portions of the extract sample, each weighing 15 mL, were selected. One of the samples was for the MIP while the other was for the NIP.

in the resultant solutions were determined using UV-vis spectrophotometer. The adsorption capacity Q$_e$

4

(mg/g) was calculated before and after the adsorption according to Eq. 1.

3. Results and discussion

3.1 Structural analysis of the MIP and NIP

3.1.1 Scanning electron microscope

SEM technique is an essential and valuable analysis for unfolding understanding on the morphology and texture of the polymers. Comparing the SEM images of pyrocatechol-MIP (leached), MIP (unleached) and NIP in Fig. 1, the surface morphologies are quite different: notwithstanding both the NIP and unleached-MIP have smoother surfaces compared to leached MIP. The unleached MIP seems to be much compressed and crammed with homogenous surface, as shown in Fig. 1A. The image in Fig. 1B for the leached-MIP exhibited a grainier, rough and sponge like surface structure than the unleached-MIP and NIP counterparts, which confirmed the presence of cavities on the MIP. The formation of the cavities has created an irregular texture on the surface of the leached-MIP which resulting excellent porosity and more open structure than that of the NIP (Fig.1C)
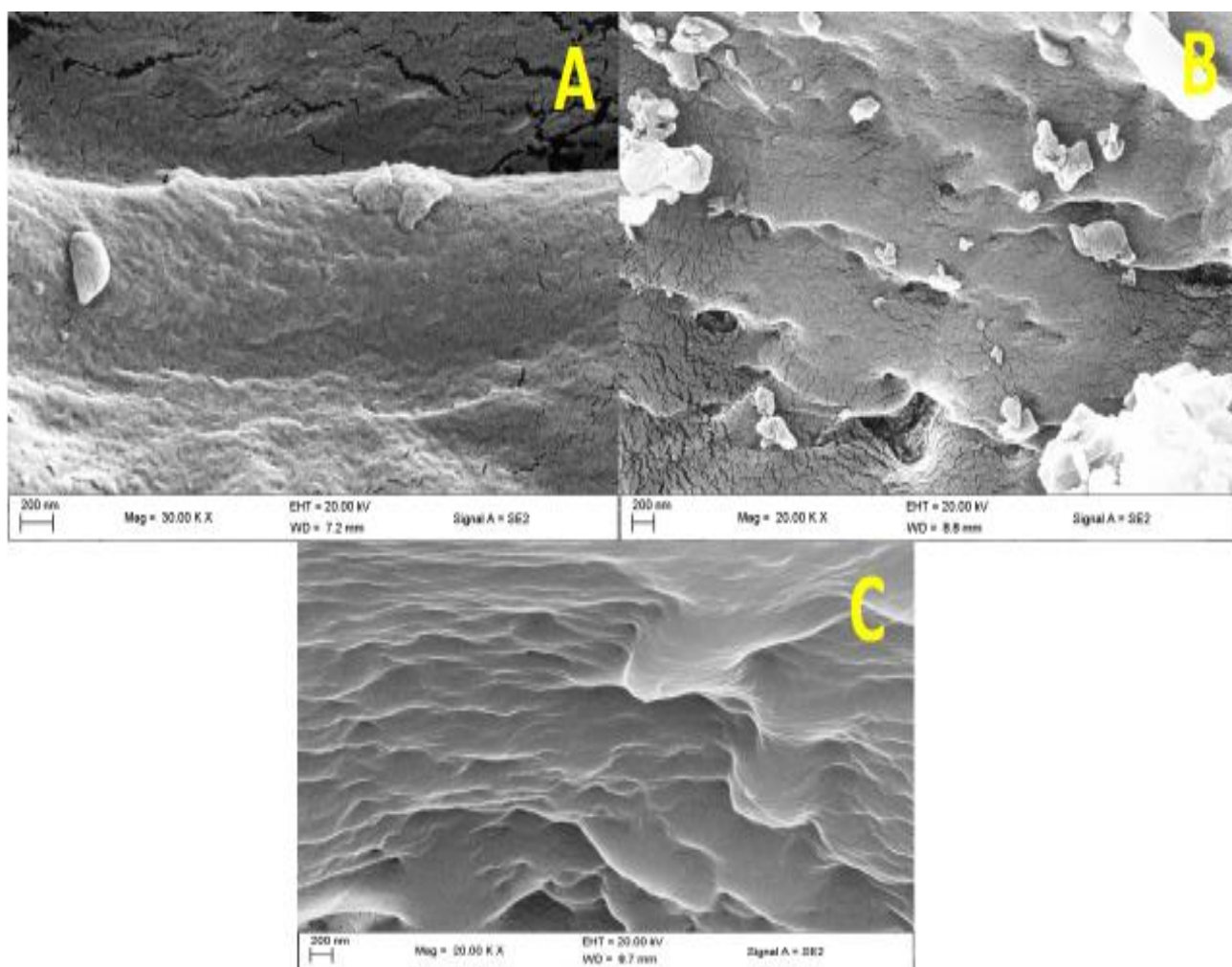

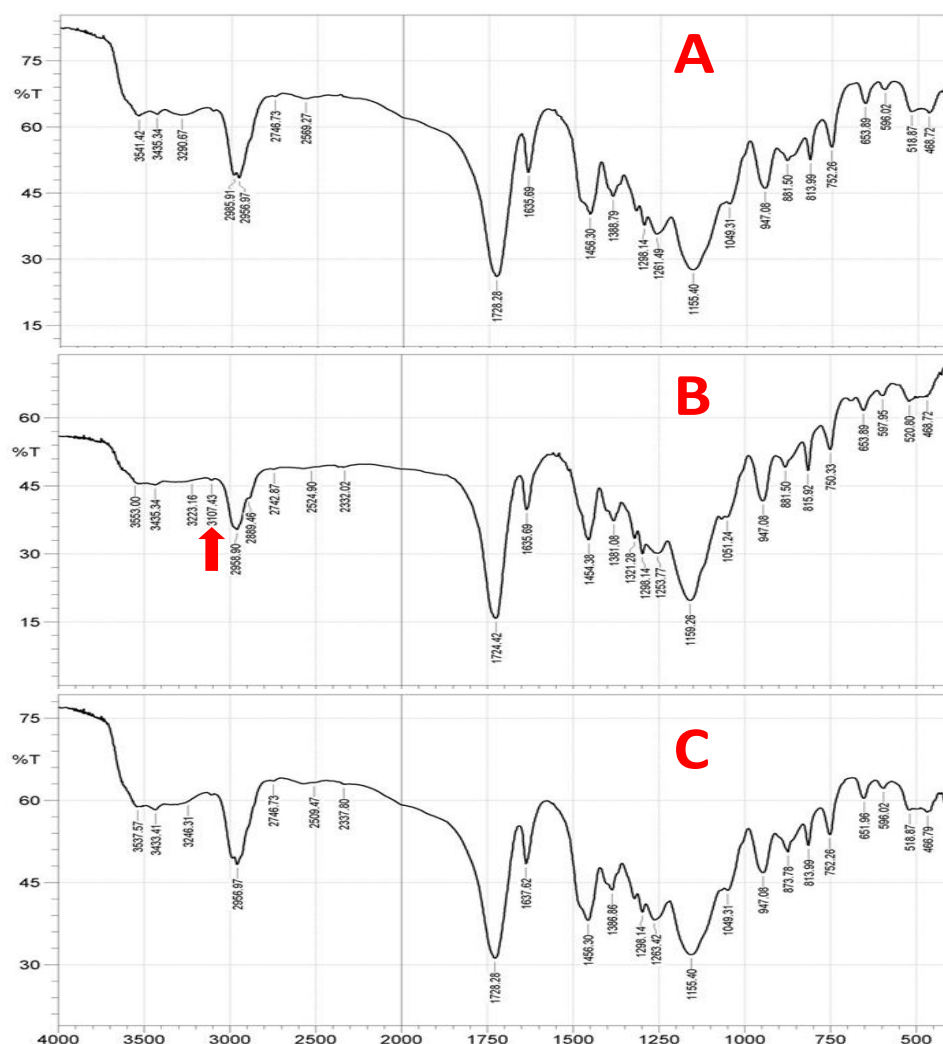**Fig. 1:** Surface morphologies of unleached-MIP (A), leached-MIP (B) and NIP (C)

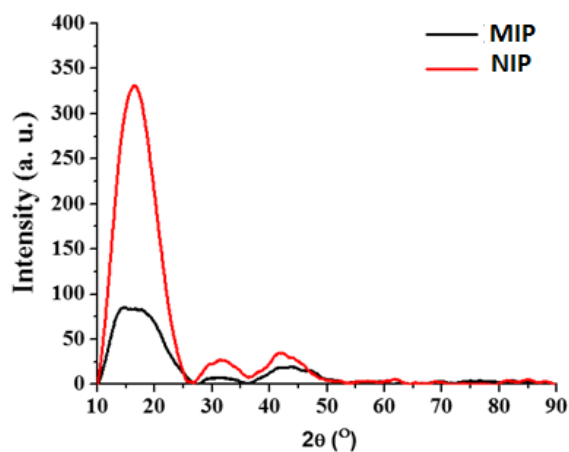**Fig.2:** FTIR spectra for **(A)** leached-MIP **(B)** unleached-MIP, and **(C)** NIP

Fig. 3: XRD diffractograms of imprinted (MIP), and non-imprinted polymer (NIP)

3.1.2 FTIR analysis

To ensure the interaction among PC, MAA and EGDMA, FTIR analysis was performed. This is crucial for determining the chemical characteristic and compositions of imprinted polymer. As shown in Fig. 2, a similar backbone was exhibited for all the polymers, and this proves that majority of the crosslinking agent (EGDMA) takes part in the reaction. The characteristic absorption bands in the range 1728 to 1724 cm^{-1} in all the polymers are assuredly ascribed to C=O stretching of the EGDMA and MAA monomer whilst that at 2985 to 2956 cm^{-1}

can be ascribed to methyl C-H stretching. The peak from 1263 to 1049 cm^{-1} is assigned to the stretching vibration of C-N in AIBN initiator. However, the main difference observed in all the spectra was the presence of an absorption peak at 3107 cm^{-1} (Fig. 2B) which could be attributed to the presence of PC with free O-H in the unleached-MIP. This band is lost in both leached-MIP and NIP- this means that imprinting has been successful. Additionally, the broad absorption bands from 3553 to 3433 cm^{-1} are assigned to OH acid of the MAA monomer, which means that there is complete polymerization of crosslinking and functional monomers.

3.1.3 X-ray Diffraction

XRD diffractograms of the NIP and MIP are demonstrated in Fig. 3. X-ray diffraction is a significant analysis for unveiling information about crystalline phases of the polymer, and to estimate the crystalline sizes. The x-ray diffractograms of both NIP and MIP materials displayed diffusive peaks at about $2\Theta = 27$ to 50° and may be attributed to amorphous phase. The maximum intensity peak at $2\Theta = 17^O$ for the NIP has been noted as the emblem peak for highly crystalline structure. It could also be observed for the imprinted polymer (MIP), the presence of broad crystalline peak in the range of $2\Theta = 13$ to 20°, exhibiting a different ordering of crystalline phase with lower intensity compared to the NIP counterpart. The lower intensity peak observed in MIP could be ascribed to the presence of template in the MIP which altered the crystal structure of the MIP and thus, indicated the formation of a new rigid structure [23].

3.2 Adsorption isotherm

The equilibrium adsorption isotherm experiments were determined in a series of PC chloroform solutions with different initial concentrations at room temperature for 6 h. In Fig. 4, the experimental results for the MIP and NIP are depicted. The adsorption capacity of the MIP increases from 1.91 to 27.60 mg/g by increasing the initial concentration of PC from 10 to 500 mg/L, yielding a hyperbolic curve. Besides, the adsorbed template quantity to the NIP

also increased with PC concentration but to a much lesser extent, with maximum adsorption amount around 19.98 mg/g. This phenomenon could be explained that the geometric factors (shape and size) of both MIP and the adsorbed molecule play an important role in the adsorption process, and thus possessed a heightened affinity for PC [24]. This result is an indicative of true molecular imprinting effect being observed with the MIP sorbent material. In order to describe the adsorption behavior of PC between the liquid and MIP phases, the experimental data were applied to empirical models. In the current study, the equilibrium data were fitted with the Langmuir and Freundlich models. Freundlich's model is considered a generalization of the Langmuir model applied to an heterogenous surface with an energy distribution corresponding to an exponential decrease [25]. Langmuir equation describes quantitatively the formation of a monolayer adsorbate on the outer surface of the adsorbent, and after that no further adsorption takes place [26]. The Langmuir isotherm is valid for monolayer adsorption onto a surface containing a finite number of identical sites. Experimentally, the plot of Ce/Qe versus Ce was applied to validate the linearized Langmuir isotherm. As indicated in Table 1 and Fig. 5, equilibrium data were in excellent agreement with Langmuir isotherm having higher correlation coefficients of $R^2 = 0.996$ and $R^2 = 0.962$ for MIP and NIP respectively. In addition, this result showed that the adsorption of PC onto MIP is a monolayer adsorption.
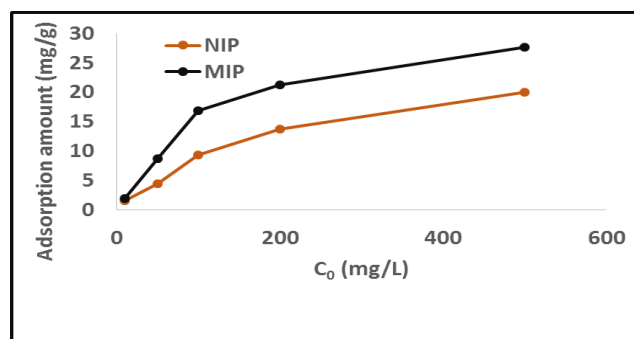

Fig.4: Adsorption isotherms of PC onto MIP and NIP at room temperature for 6 h.

Additionally, the important features of Langmuir isotherm can be expressed in terms of equilibrium

parameter R_L, which is a dimensionless constant referred to as separation factor or equilibrium parameter. The separation factor was calculated according to Eq. 4; [27].

$$R_L = \frac{1}{(1 + K_a C_0)} \qquad 4$$

where C_o (mg/L) is the initial concentration of PC, and K_a (mg/L) is Langmuir constant. The R_L value assumes the nature and the shape of the isotherm to be either unfavorable ($R_L > 1$), linear ($R_L = 1$), favorable ($0 < R_L < 1$), or irreversible ($R_L = 0$). As depicted in Table 2, the R_L values for the adsorption of PC onto MIP and NIP were in the range from 0 to 1, demonstrating that the feasibility of the adsorption was a favorable process.
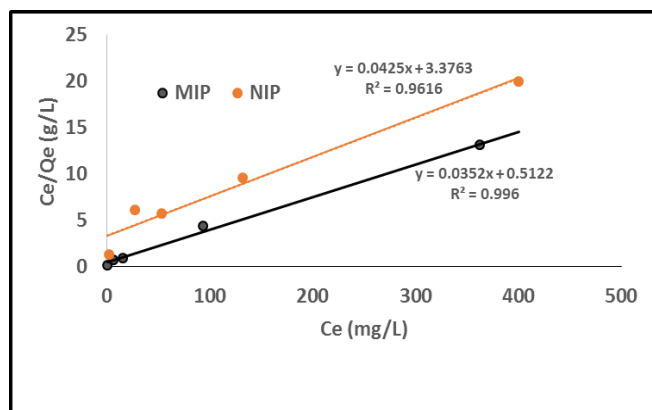

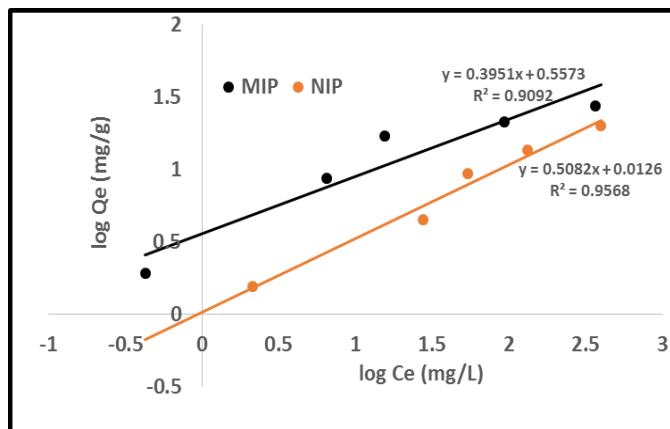**Fig.5:** Langmuir isotherm of PC adsorbed onto MIP and NIP.

Fig.6: Freundlich isotherm of PC adsorbed onto MIP and NIP.

Table 1: Parameters of Langmuir adsorption equation and Freundlich isothermal equation for adsorption experimental data.

Isotherm	Parameters	Values (MIP)	Values (NIP)
Langmuir	Qm (mg/g)	28.41	23.53
	Ka (mg/L)	0.068	0.013
	R^2	0.996	0.962
Freundlich	K_f	3.608	1.029
	n	2.531	1.968
	R^2	0.909	0.957

Table 2: R_L values based on the Langmuir equation.

C_o (mg/L)	R_L	
	MIP	NIP
10	0.595	0.885
50	0.227	0.606

100	0.128	0.435
200	0.069	0.278
500	0.029	0.133

Table 3: Evaluation of MIP/NIP performance on pharmaceutical effluent

Sample	Polymer	C_o (mg/L)	C_e (mg/L)	Adsorption capacity (mg/g)	Removal ratio (%)
Effluent	MIP	9.19	0.049	4.57	99.5
	NIP	9.19	3.500	2.85	61.9

3.3 Evaluation of MIP adsorbent performance on real effluent

Due to presence of PC in real effluents with different conditions that distinguish it from synthetic water, the MIP was applied for treating an effluent sample from pharmaceutical industry. The results before and after treatment are given in Table 3. Based on the results, it is possible to conclude that the MIP developed displayed high removal efficiency towards PC in real effluent.

4. Conclusions

As a promising technology with implicit affinity and high degree of selectivity, molecular imprinting could thus afford a dynamic complementary pathway for quantitative analysis of phenolic compounds. In this present contribution, we have evaluated molecularly imprinted polymer sorbent for binding pyrocatechol. The evident of imprinting was confirmed through FTIR analysis where broad absorption bands from 3553 to 3433 cm^{-1} were obtained. XRD analysis suggested that the presence of template in the MIP could effectively alter the crystal structure of the polymer. The MIP sorbent demonstrated outstanding affinity and showed higher molecular recognition than NIP. The mechanism of adsorption of PC on the sorbent materials followed the Langmuir adsorption isotherm. The validation of this method was carried out using an effluent from pharmaceutical industry. To this end, the efficacy of this method has great potential that could be exploited in complex sample analysis

References

[1] M.H. El-Naas, S. Al-Zuhair and M. Abu-Alhaija (2010), Removal of phenol from petroleum refinery wastewater through adsorption on date-pit activated carbon. *Chem. Eng. J,* 162, 997-1005.

[2] H. Quachtak, R. Ait Akbour, J. Douch, A. Jada and M. Hamdani (2015), Removal from water and adsorption onto natural quatz sand of hydroquinone. *J. Encap. Adsor. Sci*, 5, 131-143.

[3] A. Kumar, A. Shashi and A. Surenda (2003), Adsorption of resorcinol and catechol on granular activated carbon: Equilibrium and kinetics. *Carbon*, 41**,** 3015-3025.

[4] H. Gulley-Stahl, P.A. Hogan, W.L. Schmidt, S.J. Wall, A. Buhrlage and H.A. Bullen (2010), Surface complexation of catechol to metal oides: An ATR-FTIR, Adsorption, and Dissolution study. *Environmental Sci. & Tech*, 44, 4116-4121.

[5] S.Suresh, V.C. Srivastava, I.M. Mishra (2011), Isotherm, thermodynamics, desorption, and disposal study for the adsorption of catechol and resorcinol onto granular activated carbon. *J. Chem. & End. Data,* 56, 811-818.

[6] D. Richard, D. Schweich, M.A. Al Sawah and C. de Bellefon (2010), Depollution: A Matter of catalyst and reactor design. *Comptes Rendus Chimie*, 13, 488-493.

[7] I.N. Rodriguez, J.A.M. Leyva and J.L.H.H. Cisneros (1997), Use of a Bentonitrile-modified carbon paste electrode for the determination of some phenols in a flow system by differential-pulse voltammetry. *Analyst,* 122, 601-604.

9

[8] USEPA, technical support document for water quality based toxics control, EPA/440/485032, United States Environmental Protection Agency, Washington, DC, USA, 1985.

[9] A. Balasubramanian, S. Venkatesan (2012), Removal of phenolic compounds from aqueous solution by emulsion liquid membrane containing ionic liquid [BMIM]$^+$[PF6]$^-$ in tributyl phosphate. *Desalination,* 289, 27-34.

[10] K.Tang, L.J. Song, L.H. Duan, X.Q. Li, J.Z. Gui and Z.L Sun (2008), Deep desulfurization by selective adsorption on a heteroatoms zeolite prepared by secondary synthesis. *Fuel Process. Technol*, 89, 1−6.

[11] J. Xiao, Z. Li, B. Liu, Q.B. Xia and M.X. Yu (2008), Adsorption of benzothiophene and dibenzothiophene on ion-Impregnated activated carbons and ion-exchanged Y zeolites. *Energy Fuels,* 22, 3858−3863.

[12] B. Sellergren (2001), In: Sellergren (ed) Molecularly imprinted polymers. Man made mimics of antibodies and their applications on analytical chemistry B, Elsevier, Amsterdam, 305−322.

[13] H.Kim and D.A. Spivak (2003), New insight into modeling non-covalently imprinted polymers. *J. Am. Chem. Soc,* 125, 11269-11275.

[14] A. Beltran, F. Borrull, P.A.G. Cormack and R.M. Marcé (2010), Molecularly imprinted polymers: useful sorbents for selective extractions. *Trend in Analytical Chemistry*, 29, 1363-1375.

[15] Y. Hongyuan and H.R. Kyung (2006), Characteristic and synthesis approach of molecularly imprinted polymer. *Int. J. Mol. Sci,* 7, 155-178.

[16] K. Karim, F. Breton, R. Rouillion, E.V. Piletska, A. Guerreiro, I. Chianella and S.A. Piletsky (2005), How to find effective functional monomers for effective molecularly imprinted polymers? *Advanced Drug Delivery Reviews,* 57, 1795-1808.

[17] L. Zhang, G. Chang, C. Fu and X. Liu (2003), Tyrosine imprinted polymer beads with different functional monomers via seed swelling and suspension polymerization. *Polym. Eng. Sci,* 4, 965-974.

[18] E. Yilmaz, K. Mosbach and K Haupt (1999), Influence of functional and crosslinking monomers and the amount of template on the performance of molecularly imprinted polymers in binding assays. *Anal. Commun*, 36, 167-170.

[19] J.L. Urraca, M.C. Carbajo, M.J. Torralvo, J. Gonzales-Vasquez, G. Orellana and M.C. Moreno-Bondi (2008), Effect of the template and functional monomer on the textural properties of molecularly imprinted polymers. *Biosens. Bioelectr*, 24, 155-161.

[20] K.N. Awokoya, B.S. Batlokwa, B.A. Moronkola, S. Chigome, D.A. Ondigo, Z. Tshentu, and N.Torto (2013), Development of a styrene based molecularly imprinted polymer and its molecular recognition properties of vanadyl tetraphenylporphyrin in organic media, *Intern.J. Polym. Mat. Polym. Biomat.* 63, 107-113.

[21] D.K. Singh and S. Mishra (2010), Synthesis and characterization of Hg(II)-ion-imprinted polymer: kinetic and isotherm studies. *Desalination,* 257, 177-183.

[22] I. Langmuir (1916), The adsorption of gases on plane surface of glass, mica and platinum. *J. Am. Chem. Soc,* 40, 1361.

[23] M. Damirel, S.B. Sevin, R. Say and Y. Yazan (2007), Propranolol HCl imprinted polymeric microspheres: Development, characterization and dissolution. *FABAD J. Pharm. Sci*. 32, 147-157.

[24] I. Polyakova, L. Borovikova, A. Osipenko, E. Vlasova, B. Volchek and O. Pisarev (2016), Surface molecularly imprinted organic-inorganic polymers having affinity sites for cholesterol. *Reactive & Func. Poylm.* 109, 88-98.

[25] J.A. Garcia-Calzón and M.E. Diaz-Garcia (2007), Characterization of binding sites in molecularly imprinted polymers. *Sens. Actuators B,* 123, 1180-1194.

[26] L. Qin, X.W. He, W. Zhang, W.Y. Li and Y.K. Zhang (2009), Macroporous thermosensitive imprinted hydrogel for recognition of protein by metal coordinate interaction. *Anal. Chem,* 81, 7206-7216.

[27] X.M. Guo, X.G. Liu, B.S. Xu and T. Dou (2009), Synthesis and characterization of carbon sphere-silica core-shell structure and hollow silica spheres. *Colloids Surf. A,* 345, 141-146.